International Journal of Innovative
Computing, Information and Control
Volume **16**, Number **4**, August **2020**

ICIC International ©2020 ISSN 1349-4198
pp. 1449–1457

EFFECT OF STRAIGHTENING DISTORTION CAUSED BY RESIDUAL STRESSES ON ULTIMATE COMPRESSIVE STRENGTHS OF U-RIB STIFFENED PLATES

Jongseo Kim and Myungil Kim*

Supercomputing Modeling and Simulation Center
Korea Institute of Science and Technology Information
245, Daehak-ro, Yuseong-gu, Daejeon 34141, Korea
jskim99@kisti.re.kr; *Corresponding author: mikim@kisti.re.kr

Received January 2020; revised April 2020

Abstract. *The residual stresses resulting from a welding process in which plates and stiffeners are joined have a detrimental effect on the ultimate strength of stiffened plates and they have to be carefully analyzed. Therefore, the ultimate compressive strengths of U-rib stiffened plates with various combinations of column and plate slenderness parameters were evaluated using nonlinear Finite Element Analysis (FEA). The effect of straightening the distortion caused by the application of residual stresses on the strength of these plates was investigated. It was found that the straightening process could increase the ultimate strength up to 15% even though the displacements caused by the residual stresses could increase up to three times the initial geometric imperfection. FEA results were also compared with the strength predictions from the Federal Highway Administration (FHWA). For the stiffened plates whose plate slenderness parameters were greater than 0.9, the FHWA predictions were not conservative in the region having relatively low column slenderness parameter values.*

Keywords: Ultimate compressive strengths, Stiffened plates, U-rib, Residual stresses, Initial geometric imperfection, Straightening distortion, FHWA

1. **Introduction.** Stiffened steel plates having a high strength-to-weight ratio are widely used in a variety of engineering structures such as bridges, ships and offshore structures; this is because the addition of a few stiffeners to the plates produces considerably stiffer systems [1]. Currently, in addition to open-type stiffeners, U-rib stiffeners with excellent torsional rigidity are also frequently used in engineering applications [2].

To predict the accurate in-plane ultimate compressive strength of these stiffened plates through numerical computations, ultimate strength analysis based on geometric and material nonlinear Finite Element Analysis (FEA) should be conducted considering the initial geometric imperfections and residual stresses [3].

In particular, the residual stresses resulting from a welding process in which plates and stiffeners are joined have a detrimental effect on the ultimate strength; therefore, attention should be paid to not only the residual stress themselves but also to the distortions caused by these stresses in numerical analyses. So far, many researchers have investigated the inherent strain, which is regarded as the source of residual stresses, through welding simulations based on thermal elastic-plastic FEA, and applied it to the assembly of structures to predict residual stresses and welding distortions [4-6]. In addition, they have focused on minimizing distortions through reverse designing, which finds pre-cambering shapes and magnitudes beforehand.

DOI: 10.24507/ijicic.16.04.1449

However, precise prediction of welding residual stresses and distortions for large structures through numerical simulation is still not easy because of the high computational cost. Moreover, engineers are occasionally equipped with insufficient information for welding in practical design. Therefore, many researchers have performed ultimate strength analysis using idealized residual stress models [7,8]. This study reexamines the techniques for dealing with the stress models required for numerical analysis.

Figure 1 shows typical residual stress patterns commonly used in numerical analysis. Unlike the third pattern, the first and second patterns cannot meet the moment equilibrium requirements with respect to the neutral axis owing to their asymmetric geometry even if the force equilibrium is satisfied. Hence, the application of residual stresses distorts the initial shapes of the stiffened plates and affects the ultimate strength. To be precise, the ultimate strength depends on whether straightening processes are carried out.

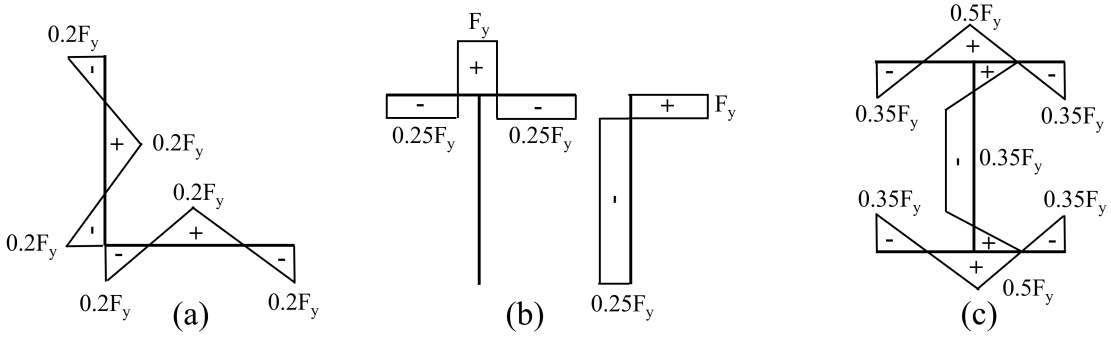

FIGURE 1. Typical residual stress patterns

Basically, two previous approaches, one using a perfect system [9] and the other using an imperfect system [10], have been used in the straightening processes, and both of them applied fictitious temperature changes corresponding to the residual stresses on stiffened plates. In recent studies, residual stress models are directly applied to stiffened plates based on the initial conditions for analyzing the ultimate strength [7,8,11,12]; however, the effects of the straightening process on the ultimate strength have not been analyzed adequately. Therefore, this study analyzed the effects of the straightening process on the ultimate compressive strength of U-rib stiffened plates by applying a residual stress model.

Regarding the ultimate compressive strength of stiffened plates, the Federal Highway Administration (FHWA) provided a strength predictor diagram that could predict the strength of the plates with two simple slenderness parameters [13,14]. Owing to its simple yet precise strength prediction, this diagram is widely utilized in designing bridges. This study also evaluated the FHWA strength predictor diagram by comparing it with FEA results.

2. Incorporation of Residual Stresses in FE Analysis.

Previous approaches used a temperature change corresponding to residual stresses for the straightening process. For a simpler and more convenient approach, the residual stresses themselves could be directly used in the straightening process (hereinafter current approach).

To identify differences in the previous and present load-displacement (hereinafter LD) curves, a preliminary study based on the perfect system was carried out using the same stiffened plates as those used in Sheikh's FE analysis shown in Figure 2. The model details [9] are summarized in Table 1. Here, L_u, f_{yp} and f_{ys} represent the longitudinal length of the stiffened plates, yield strength of the plates and that of the stiffeners, respectively.

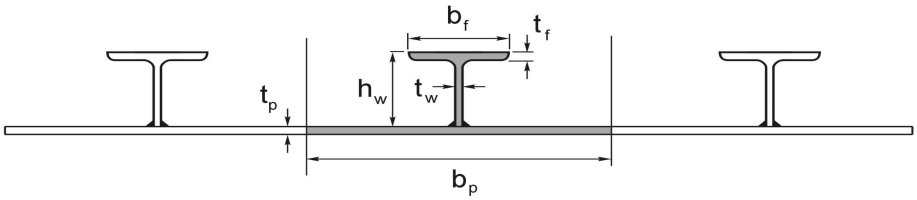

FIGURE 2. The stiffened plate used in Sheikh's study

TABLE 1. Geometry and material property of the Sheikh's model (unit: mm, MPa)

Model ID	b_p	h_w	b_f	t_p	t_w	t_f	L_u	f_{yp}	f_{ys}
t_p_PB	702	150	135	16	12	12	1264	420	420

The others denote each dimension of the model. The study results revealed no significant difference in the LD curves. Thus, this study used the residual stress model directly for the straightening process.

An additional preliminary study was performed to identify differences in the ultimate compressive strengths obtained using a perfect system and an imperfect system. The first method using a perfect system involved the following three steps. Step 1. The negative of the desired residual stresses is applied to a perfect system. Step 2. The displacements produced in Step 1 are added to the desired geometric imperfection to generate stress-free meshes. Step 3. The desired residual stresses are applied to the stress-free meshes produced in Step 2 and the equilibrium is determined. After establishing the equilibrium, axial compressions are applied to the stiffened plates. Similar to the first method, the second method using an imperfect system also involved the following three steps. Step 1. The negative of the desired residual stresses is applied to an imperfect system. Step 2. Stress-free meshes are generated. Step 3. The desired residual stresses are applied to the stress-free meshes produced in Step 2 and the equilibrium is determined. The next step is the same as that in the first method. The second method is more complicated compared to the first one in terms of implementing the straightening process. Figure 4 schematically illustrates the first and second methods. The additional preliminary study

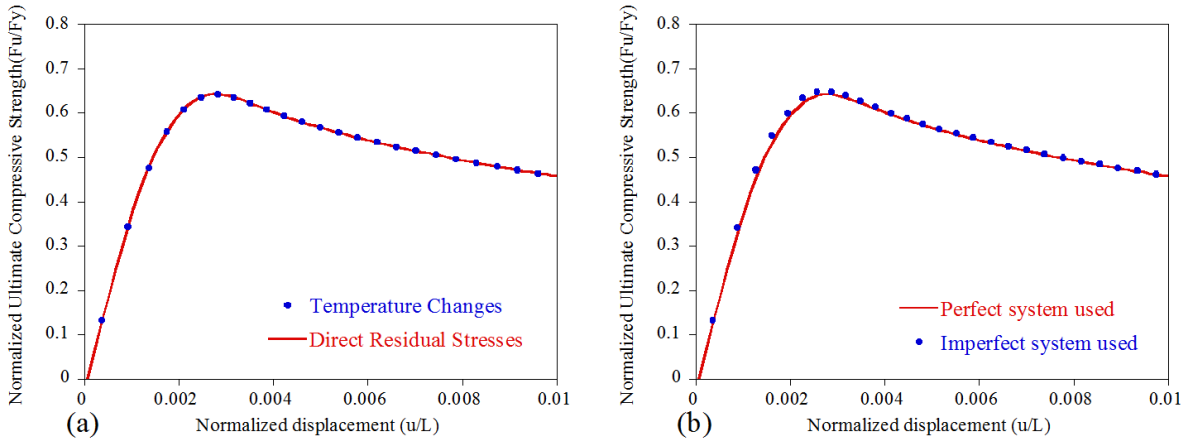

FIGURE 3. Comparison between LD curves obtained through (a) the temperature changes & the direct residual stresses, and through (b) the perfect system and the imperfect system

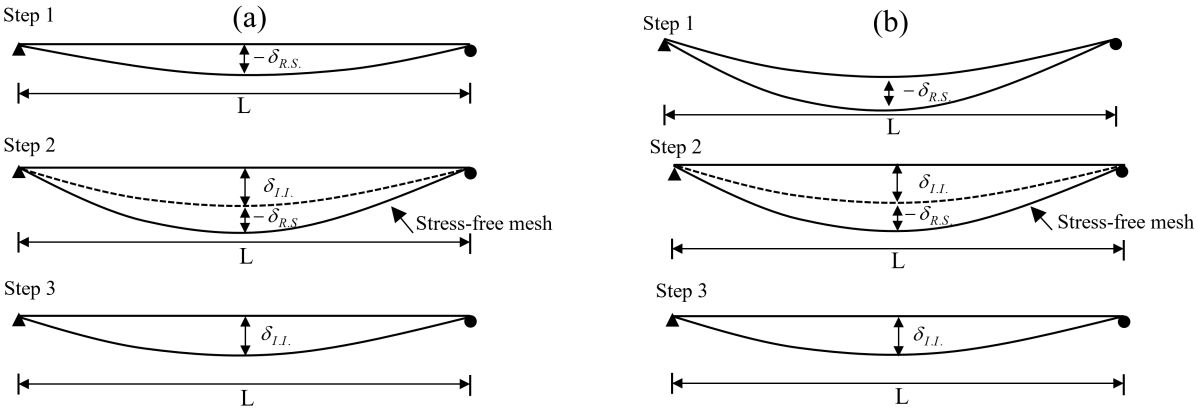

FIGURE 4. The straightening process using (a) a perfect system and (b) an imperfect system

also revealed no significant difference in the LD curves obtained through the above two methods as shown in Figure 3(b). Therefore, the first method using a perfect system was used in the rest of this study to apply the residual stresses.

3. FE Analysis for U-rib Stiffened Plates.

3.1. **Geometry and material property of analysis models.** The analysis model used in this study is a stiffened plate system composed of a skin plate and ten longitudinal U-ribs as shown in Figure 5. B and L denote the width and length of the hypothetical model, respectively. The geometrical details are summarized in Table 2.

According to the FHWA [13], the normalized ultimate compressive strength of the stiffened plates, F_u/F_y, is considered a function of the plate slenderness parameter, λ_{pl},

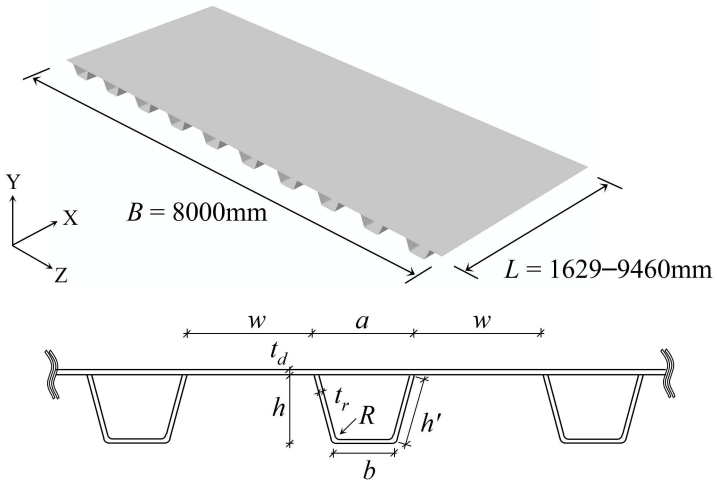

FIGURE 5. Stiffened plates with U-ribs

TABLE 2. Geometry of the stiffened plates (unit: mm)

U-rib type	a	w	b	h	h'	R	t_r	t_d	L
$400 \times 240 \times 8$	400	400	250	240	251	40	8	7-30	1629-9460

and column slenderness parameter, λ_{col}, and calculated as follows:

$$\frac{F_u}{F_y} = f(\lambda_{pl}, \lambda_{col}), \text{ where } \lambda_{pl} = \frac{w/t_d}{1.9}\sqrt{\frac{F_y}{E}} \text{ and } \lambda_{col} = \frac{1}{\pi}\sqrt{\frac{F_y}{E}}\frac{L}{r} \tag{1}$$

where f denotes the interaction diagram, F_u and F_y are the ultimate compressive strength and yield strength of stiffened plates, w, t_d, L, r, and E represent the spacing of the longitudinal stiffeners, thickness of a flange plate, length of the longitudinal stiffeners, radius of gyration of stiffener struts and the elastic modulus of stiffened plates, respectively. Only two design variables, t_d and L, which were determined from predefined values of the slenderness parameters are independent variables in this study. To consider material nonlinearity, SM490Y steel was modeled as the elastic-plastic strain-hardening material, as shown in Figure 6. The mechanical properties of SM490Y are summarized in Table 3.

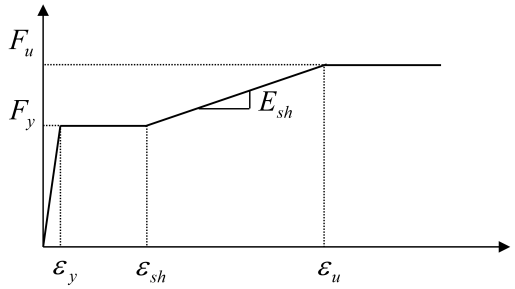

FIGURE 6. Stress-strain relationship

TABLE 3. Mechanical properties of SM490Y

E (GPa)	F_y (MPa)	F_u (MPa)	ε_y	ε_{sh}	ε_u	E_{sh} (MPa)
200	355	490	0.0018	0.0210	0.0585	3600

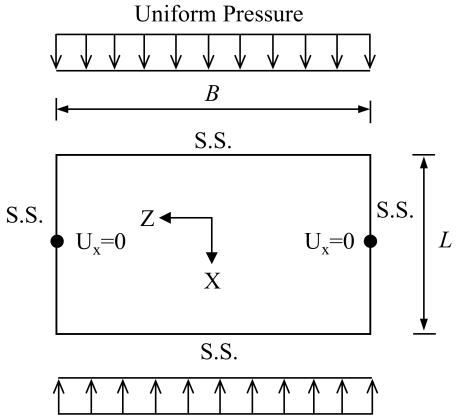

FIGURE 7. Boundary condition of the stiffened plate

3.2. **FE modeling and simulation.** The FE program ABAQUS version 6.14 [15] was utilized in FE modeling and simulation. The stiffened plate was modeled using S4R5 (four-node rectangular shell) elements. All sides of the stiffened plate were assumed as simple supports. In addition, the two points marked with black spots in Figure 7 were constrained in the longitudinal direction ($U_x = 0$) to prevent structural instability. Uniform axial compressions were applied to both transverse edges of the stiffened plate as

shown in Figure 7. To trace the nonlinear equilibrium path under increasing compressive forces, the modified Riks method was used.

The initial geometric imperfection significantly influences the ultimate strength. In this study, the column-type buckling mode, shown in Figure 8, was incorporated in FEA. The magnitude of the maximum deflection (scaling factor), $\delta_{I.I.}$, was assumed as $L/1000$ referring to the Structural Stability Research Council (SSRC) column curve [3]. Figure 9 shows the residual stress pattern assumed in this study, which was suggested by Fukumoto et al. [16] and has been used in many studies [11,12].

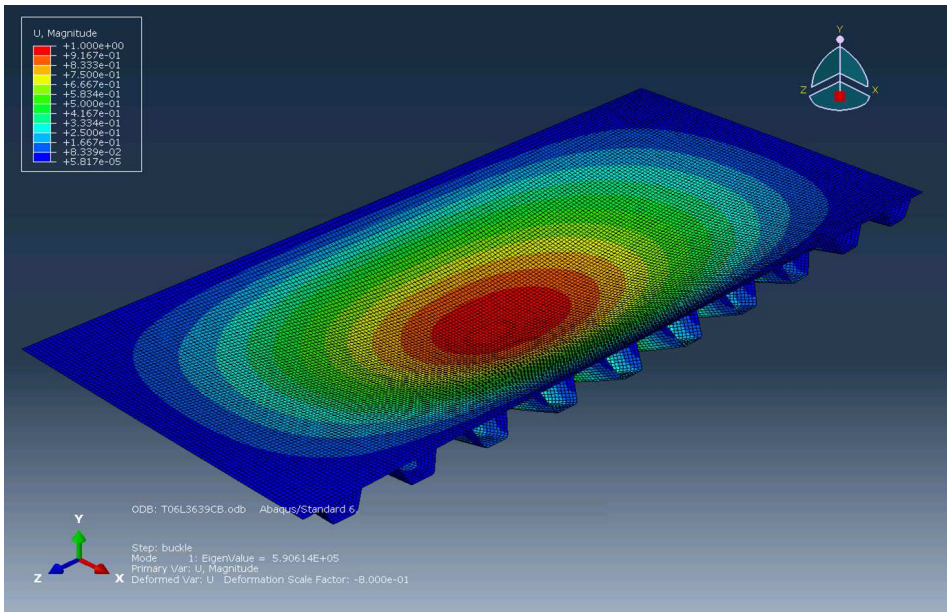

FIGURE 8. (color online) Initial imperfection mode

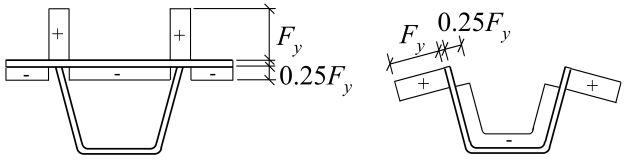

FIGURE 9. Residual stress pattern

4. **FE Analysis Results and Discussion.** The geometric and material nonlinear FE analyses for the stiffened plates were conducted and the results obtained are summarized in Table 4. In Table 4, $\delta_{\max}$ denotes the resulting vertical displacements (Y direction in Figure 5) caused by residual stresses in the stress redistribution step; SO and SX denote the ultimate compressive strengths including and excluding the straightening process, respectively. In addition, strength increase was calculated as (SO−SX)/SX and expressed as a percentage. In the last column, FHWA/SO is the ratio of the FHWA strength to the SO strength. It is evident that the FHWA strength is conservative compared to the FEA strength when the FHWA/SO values are less than 1 (one).

It was observed that the displacement ($\delta_{\max}$) caused by the application of residual stresses increased significantly for long stiffened plates. In some cases, the imperfection ratio ($\delta_{\max}/L$) was thrice the initial geometric imperfection ratio ($\delta_{I.I.}/L$) as shown in Figure 10.

TABLE 4. FE analysis results for the hypothetical models

Model	λ_{pl}	λ_{col}	t_d (mm)	L (mm)	$\delta_{\max}$ (mm)	Ultimate compressive strength F_u/F_y SX (no straightening)	SO (straightening)	Strength Increase (%)	FHWA/SO
A-1	0.3	0.3	30	1629	−0.8	1.001	0.996	−0.5	0.955
A-2		0.5		2716	−2.0	0.974	0.987	1.3	0.890
A-3		0.7		3802	−3.8	0.836	0.860	2.9	0.913
A-4		0.9		4888	−6.1	0.714	0.752	5.3	0.894
A-5		1.1		5975	−8.7	0.637	0.675	6.0	0.815
A-6		1.3		7061	−11.2	0.588	0.625	6.3	0.704
B-1	0.5	0.3	18	1878	−1.1	0.994	0.988	−0.6	0.963
B-2		0.5		3131	−2.8	0.924	0.944	2.2	0.931
B-3		0.7		4383	−5.5	0.787	0.817	3.8	0.961
B-4		0.9		5635	−8.9	0.698	0.731	4.7	0.919
B-5		1.1		6887	−12.4	0.630	0.668	6.0	0.823
B-6		1.3		8140	−15.8	0.585	0.628	7.4	0.701
C-1	0.7	0.3	13	2018	−1.4	0.894	0.914	2.2	0.933
C-2		0.5		3364	−3.6	0.888	0.913	2.8	0.882
C-3		0.7		4709	−6.9	0.753	0.788	4.7	0.955
C-4		0.9		6055	−11.2	0.668	0.707	5.9	0.950
C-5		1.1		7400	−15.6	0.608	0.649	6.7	0.847
C-6		1.3		8746	−19.8	0.567	0.612	7.9	0.719
D-1	0.9	0.3	10	2101	−1.7	0.717	0.712	−0.7	1.075
D-2		0.5		3502	−4.1	0.673	0.694	3.1	1.029
D-3		0.7		4903	−8.1	0.661	0.684	3.5	0.962
D-4		0.9		6304	−13.1	0.638	0.680	6.9	0.869
D-5		1.1		7705	−18.5	0.567	0.621	9.5	0.831
D-6		1.3		9106	−23.6	0.528	0.587	11.2	0.750
E-1	1.1	0.3	8	2152	−1.8	0.664	0.679	2.3	1.008
E-2		0.5		3587	−4.6	0.608	0.635	4.4	1.000
E-3		0.7		5022	−9.1	0.519	0.588	13.3	0.987
E-4		0.9		6457	−14.8	0.481	0.555	15.4	0.939
E-5		1.1		7891	−21.1	0.479	0.542	13.2	0.845
E-6		1.3		9326	−27.1	0.471	0.537	14.0	0.737
F-1	1.3	0.3	7	2183	−1.9	0.638	0.645	1.1	0.958
F-2		0.5		3639	−5.0	0.587	0.555	−5.5	1.033
F-3		0.7		5094	−9.9	0.523	0.559	6.9	0.938
F-4		0.9		6549	−16.2	0.457	0.505	10.5	0.925
F-5		1.1		8005	−23.3	0.402	0.459	14.2	0.887
F-6		1.3		9460	−30.3	0.395	0.443	12.2	0.804

Table 4 showed that the SO method could provide a strength increase up to 15% compared to the SX method. In addition, the SO method showed strong effects on the strength where λ_{col} were relatively large. This means the SX method provided conservative strength estimates in those regions. In case of steel bridges, strengths increases of 3-4% are expected because the models used practically are C-2 and C-3 [17].

As observed in Table 4, FHWA strengths are less than those determined via FE analysis, where λ_{pl} is less than 0.7. The ratio of the FHWA strength to the SO strength is in the range 0.701-0.963. However, the models for which λ_{pl} is greater than 0.9 showed that the FHWA strength predictions were not conservative in the region where column slenderness parameters are relatively small. Therefore, caution is required when using FHWA predictions in the regions with relatively small column slenderness parameters.

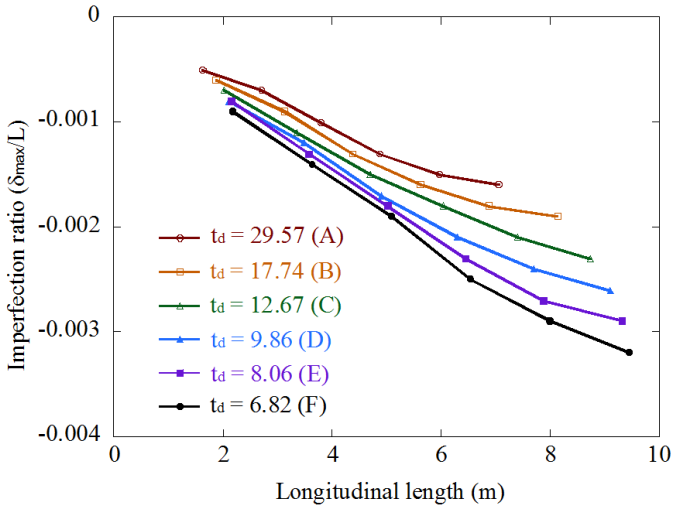

FIGURE 10. Additional initial geometric imperfection generated by residual stresses

5. **Conclusion.** The effects of the straightening the distortions caused by the application of residual stresses on the ultimate compressive strength of U-rib stiffened plates were quantitatively evaluated based on a numerical method using the commercial FEA program ABAQUS. Totally 36 hypothetical models with various combinations of column and plate slenderness parameters were developed, and ultimate strength analysis based on geometric and material nonlinearity using FEA was conducted incorporating initial geometric imperfections and residual stresses.

In this study, it was confirmed that the fictitious temperature changes corresponding to the residual stresses and direct use of the residual stresses in the straightening process provided almost identical results. In addition, there was no significant difference in the LD curves obtained through a perfect system and an imperfect system. Based on these results, the straightening process was carried out through the direct use of residual stresses and the perfect system.

It was observed that the displacement caused by the application of residual stresses increased up to three times the value of $L/1000$. The strengths obtained in the straightening process gradually increased when λ_{col} increased. The straightening process could provide strength increases up to 15%. The FHWA strength predictions appeared to be generally conservative. However, the models for which λ_{pl} was greater than 0.9 showed that FHWA strength predictions were not conservative. Therefore, caution is required when using FHWA predictions in regions where column slenderness parameters are relatively small.

This study evaluated effects of the straightening process on the ultimate strength for the residual stress model proposed by Fukumoto et al. In the future, it is necessary to confirm the effects for various residual stress models.

Acknowledgment. This research (2019) was supported by Korea Institute of Science and Technology Information (KISTI).

REFERENCES

[1] C. Li, S. Dong, T. Wang, W. Xu and X. Zhou, Numerical investigation on ultimate compressive strength of welded stiffened plates built by steel grades of S235-S390, *Appl. Sci.*, vol.9, no.10, 2019.

[2] J. S. Kim and K. Kim, Strength interaction of wide steel box girder subjected to concurrent action of compression and flexure for cable-supported bridges, *Journal of Korean Society of Steel Construction*, vol.31, no.4, pp.301-309, 2019 (in Korean).

[3] R. D. Ziemian, *Guide to Stability Design Criteria for Metal Structures*, 6th Edition, Wiley, 2010.

[4] D. Deng, H. Murakawa and W. Liang, Numerical simulation of welding distortion in large structures, *Computer Methods in Appl. Mech. and Eng.*, vol.196, nos.45-48, pp.4613-4627, 2007.
[5] H. Murakawa, D. Deng and N. Ma, Concept of inherent strain, inherent stress, inherent deformation and inherent force for prediction of welding distortion and residual stress, *Trans. of JWRI*, vol.39, no.2, 2010.
[6] J. Wang, S. Rashed, H. Murakawa and Y. Luo, Numerical prediction and mitigation of out-of-plane welding distortion in ship panel structure by elastic FE analysis, *Mar. Struc.*, vol.34, pp.135-155, 2013.
[7] D. K. Shin, V. A. Le and K. Kim, In-plane ultimate compressive strength of HPS deck panel system stiffened with U-shaped ribs, *Thin Walled Structures*, vol.63, pp.70-81, 2013.
[8] K. Kim, In-plane compressive strength of hybrid steel stiffened plate with single stiffener, *Journal of Korean Society of Steel Construction*, vol.31, no.1, pp.65-73, 2019 (in Korean).
[9] I. A. Sheikh, G. Y. Grondin and A. E. Elwi, *Stiffener Tripping in Stiffened Steel Plates*, Structural Engineering Report No. 236, Dep. of Civil and Env. Engineering, University of Alberta, 2001.
[10] E. C. L. Wang, G. Y. Grondin and A. E. Elwi, *Interaction Buckling Failure of Stiffened Steel Plates*, Structural Engineering Report No. 264, Dep. of Civil and Env. Engineering, University of Alberta, 2006.
[11] C. C. Chou, C. M. Uang and F. Seible, Experimental evaluation of compressive behavior of orthotropic steel plates for the new San Francisco Oakland Bay bridge, *J. of Bridge Eng.*, vol.11, no.2, pp.140-150, 2006.
[12] D. K. Shin, B. V. Dat and K. Kim, Compressive strength of HPS box girder flanges stiffened with open ribs, *Journal of Constructional Steel Research*, vol,95, no.4, pp.230-241, 2014.
[13] R. Wolchuck and R. M. Mayrbourl, *Proposed Design Specification for Steel Box Girder Bridges*, Report No. FHWA-TS-80-205, Federal Highway Administration, Washington, D.C., 1980.
[14] Federal Highway Administration, *Manual for Design, Construction, and Maintenance of Orthotropic Steel Deck Bridges*, Report No. FHWA-IF-12-027, 2012.
[15] ABAQS Inc., *ABAQUS Standard User's Manual. Ver. 6.14*, 2014.
[16] Y. Fukumoto, T. Usami and Y. Okamoto, Ultimate compressive strength of stiffened plates, *Proc. of Specialty Conf. on Metal Bridge*, St. Louis, MO, 1974.
[17] Incheon Bridge Co., *Structural Engineering Report*, 2009.